Realization of High-Energy Emission from $[Cu(N-N)(P-P)]^+$ Complexes for Organic Light-Emitting Diode Applications

Liming Zhang,[†,‡] Bin Li,[*,†] and Zhongmin Su[§]

Key Laboratory of Excited State Processes, Changchun Institute of Optics Fine Mechanics and Physics, Chinese Academy of Sciences, Changchun 130033, P. R. China, Graduate School of the Chinese Academy of Sciences, Chinese Academy of Sciences, Beijing 100039, P. R. China, and Department of Chemistry, Northeast Normal University, Changchun 130024, P. R. China

Received: April 24, 2009; Revised Manuscript Received: June 21, 2009

In this paper, we propose a potential method leading to high-energy emitting Cu(I) complexes. Diimine ligands with high-π^* and their corresponding $[Cu(N-N)(P-P)]BF_4$ complexes are synthesized. Systematic research proves that the utilization of diimine ligands with high-π^* is a practicable and effective method to lead to high-energy emission from $[Cu(N-N)(P-P)]BF_4$ complexes. Efficient blue- and green-emitters are realized, and their electroluminescence (EL) performances are also investigated. A maximum brightness of 2850 cd/m^2 is achieved for the blue-emitting EL device, with an emission peaking at 480 nm. Meanwhile, the green-emitting EL device reaches a maximum brightness of 2320 cd/m^2, with an emission peaking at 532 nm.

Introduction

Phosphorescent Cu(I) complexes, as a new class of electroluminescence materials for organic light-emitting diode (OLED) applications, have recently attracted much attention because of their advantages such as abundance and low cost in comparison with other heavy metal complexes.[1,2] To date, various phosphorescent Cu(I) complexes have been synthesized, and their emission properties have been qualitatively discussed.[3−6] In exploring high-efficiency phosphorescent Cu(I)-based emitters and moving toward materials with a requirement for full-color displays, many efforts have been devoted to tricolor emitters. However, the design and preparation of practicable blue emitters have been experiencing considerable challenges. This task is far more difficult than those for preparing green- and red-emitting complexes. Until now, most of the emissions localize in the low-energy region, preventing Cu(I)-based emitters from actual utilization in the fields of full-color displays and so on.[3,7−12] Thus, one of the major problems phosphorescent Cu(I)-based emitters face is the exploration of high-energy-emitting Cu(I) complexes.

Generally, emission signals from the charge−transfer (CT) excited state of Cu(I) complexes is typically weak and short-lived because the lowest-energy CT state of a d^{10} system involves excitation from a metal−ligand dσ^* orbital.[13−15] An important consequence is that the excited state typically prefers a tetragonally flattened geometry, whereas the ground state usually adopts a more tetrahedral-like coordination geometry that is appropriate for a closed-shell ion. Aside from reducing the energy content, the geometry distortion that occurs in the excited state facilitates relaxation back to ground state.[16−18] McMillin first reported this type of luminescence quenching, and by now, many other studies have confirmed this mechanism.[11,14,15] Recently, a series of new mixed ligand copper(I) polypyridine and phenanthroline complexes such as $[Cu(N-N)(POP)]^+$ [POP = bis(2-(diphenylphosphanyl)phenyl) ether], which are superior emitters, have been reported.[19−21] It is found that solvent-induced exciplex quenching is relatively inefficient for the CT excited state of this POP system. In addition, the introduction of sterically blocking ligands can impede geometry distortion as well as solvent attack. Here, the steric effect cooperates to effectively block the excited state close to ground-state geometry, which has been proved by a theoretical study conducted by Feng and co-workers on the $[Cu(N-N)(P-P)]^+$ system.[22] For a typical phosphorescent $[Cu(N-N)(P-P)]^+$ complex, the highest occupied molecular orbital (HOMO) has a predominant metal Cu d character, admixed with contributions from the phosphorus ligand, while the lowest unoccupied molecular orbital (LUMO) is essentially the π^* orbital localized on a diimine ligand. The photoluminescence corresponds to the lowest triplet T_1 and is thus assigned as a character of metal-to-ligand charge−transfer ^{3}MLCT [d(Cu) → π^*(diimine ligand)].

Guided by the above research results, it is expected that besides the utilization of sterically blocking ligands, improving the diimine ligand π^* orbital may be another method leading to high-energy emitting $[Cu(N-N)(P-P)]^+$ complexes. In this paper, we focus on diimine ligands with high-π^* and their corresponding $[Cu(N-N)(POP)]BF_4$ complexes. Systematic research confirms that the utilization of diimine ligands with high-π^* is a practicable method leading to high-energy emission from $[Cu(N-N)(POP)]BF_4$ complexes. Blue- and green-emitters are realized, and their electroluminescence (EL) performances are also investigated.

Experimental Section

The molecular structures of diimine ligands and their corresponding Cu(I) complexes are shown in Scheme 1.

2-Thiazol-4-yl-1H-benzoimidazole (Tbzimda), 2-pyridin-2-yl-1H-benzoimidazole (Pbzimda), bis[2-(diphenylphosphanyl) phenyl] ether (POP), 4,4′,4″-tri[3-methylphenylphenylamino] triphenylamine (*m*-MTDATA), 4,7-diphenyl-1,10-phenanthroline (Bphen), 4,4′-bis[N-(1-naphthyl)-N-phenylamino] biphenyl (NPB), 4,4′-dicarbazolyl-1,1′-biphenyl (CBP), tris(8-hydroxy-

* To whom correspondence should be addressed. E-mail: lib020@ciomp.ac.cn. Telephone/Fax: +86431 86176935.
† Key Laboratory of Excited State Processes, Chinese Academy of Sciences.
‡ Graduate School of the Chinese Academy of Sciences.
§ Northeast Normal University.

10.1021/jp903774g CCC: $40.75
Published on Web 07/09/2009

SCHEME 1: Molecular Structures of Diimine Ligands and Their Corresponding Cu(I) Complexes

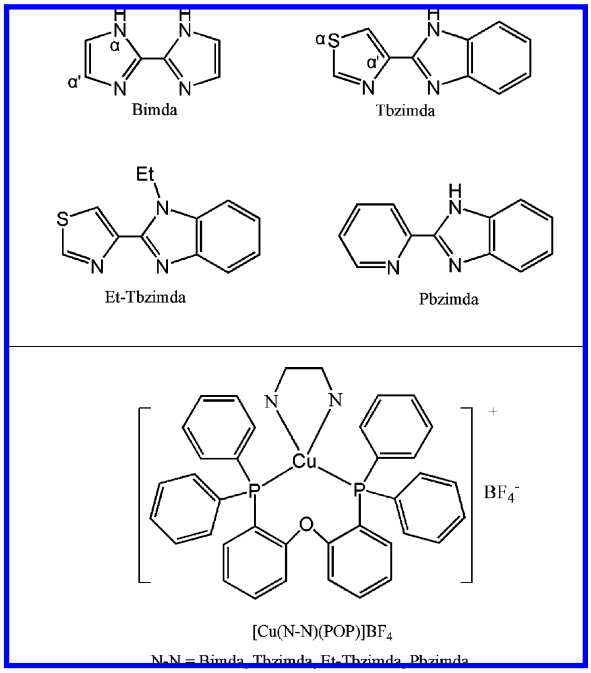

quinoline)aluminum (AlQ), LiF, and $Cu(BF_4)_2$ were purchased from Aldrich Chemical Co. and used without further purification. Solvents were freshly distilled over appropriate drying regents under an N_2 atmosphere.

Synthesis of Ligands. 1H,1′H-[2,2′]Biimidazolyl (Bimda) was synthesized according to the literature procedure.[23]

1-Ethyl-2-thiazol-4-yl-1H-benzoimidazole (Et-Tbzimda). 0.40 g (0.01 mol) NaOH and 2.01 g (0.01 mol) of Tbzimda were added to 100 mL of stirring anhydrous DMF in a 250 mL flask. 0.82 mL (0.011 mol) of bromo-ethane was then added when the solution was clear. The mixture was continually stirred for 24 h and then poured into 300 mL of cool water. The organic components were extracted with CH_2Cl_2 to yield 2.70 g white block crystals (80%). ^{1}H NMR ($CDCl_3$): δ 8.01−7.94 (m, 4H), 7.35−7.29 (m, Ar−H, 2H), 4.79−4.74 (m, C−H, 2H), 1.50 (t, 3H). Anal. Calcd for $C_{12}H_{11}N_3S$: C, 62.86; H, 4.84; N, 18.33. Found: C, 62.71; H, 4.95; N, 18.51.

Synthesis of [Cu(N−N)(POP)]BF_4. All $[Cu(N-N)(POP)]BF_4$ complexes were synthesized according to a well-known literature procedure.[21] Their identities were confirmed by NMR, elemental analysis, and single crystal XRD.

$[Cu(Bimda)(POP)]BF_4$: white powder. ^{1}H NMR ($CDCl_3$): δ 11.24 (s, N−H, 2H), 7.86−7.60 (m, Ar−H, 22H), 7.32−7.21 (m, Ar−H, 10H). ^{31}P NMR δ + 1.24 (s, $P(C_6H_5)_2C_6H_4$). Anal. Calcd for $C_{42}H_{34}BCuF_4N_4OP_2$: C, 61.29; H, 4.16; N, 6.81. Found: C, 61.01; H, 4.34; N, 7.01.

$[Cu(Tbzimda)(POP)]BF_4$: white powder. ^{1}H NMR ($CDCl_3$): δ 11.12 (s, N−H, 1H), 8.01−7.73 (m, Ar−H, 22H), 7.58−7.27 (m, Ar−H, 12H). ^{31}P NMR δ + 1.45 (s, $P(C_6H_5)_2C_6H_4$). Anal. Calcd for $C_{46}H_{35}BCuF_4N_3OP_2S$: C, 62.07; H, 3.96; N, 4.72. Found: C, 61.84; H, 4.21; N, 4.51.

$[Cu(Et\text{-}Tbzimda)(POP)]BF_4$: white powder. ^{1}H NMR ($CDCl_3$): δ 7.98−7.69 (m, Ar−H, 22H), 7.54−7.21 (m, Ar−H, 12H), 4.16−4.12 (m, C−H, 2H), 1.89−1.86 (m, C−H, 3H). ^{31}P NMR δ + 1.44 (s, $P(C_6H_5)_2C_6H_4$). Anal. Calcd for $C_{48}H_{39}BCuF_4N_3OP_2S$: C, 62.79; H, 4.28; N, 4.58. Found: C, 62.61; H, 4.35; N, 4.66. The molecular structure is further confirmed by single crystal XRD (Supporting Information).

$[Cu(Pbzimda)(POP)]BF_4$: yellow powder. δ 10.89 (s, N−H, 1H), 8.21−7.78 (m, Ar−H, 24H), 7.64−7.51 (m, Ar−H, 12H). ^{31}P NMR δ + 1.37 (s, $P(C_6H_5)_2C_6H_4$). Anal. Calcd for $C_{48}H_{37}BCuF_4N_3OP_2$: C, 65.21; H, 4.22; N, 4.75. Found: C, 65.13; H, 4.31; N, 4.59. The molecular structure is further confirmed by single crystal XRD (Supporting Information).

Methods and Measurements. Density functional theory (DFT) calculations were performed on the four diimine ligands, Bimda, Tbzimda, Et-Tbzimda, and Pbzimda, at RB3LYP/6-31G(d) level. Singlet excitation calculations on $[Cu(Et\text{-}Tbzimda)(POP)]BF_4$ and $[Cu(Pbzimda)(POP)]BF_4$ were performed by time-dependent density functional theory (TD-DFT) at RB3PW91/SBKJC level. The initial geometries were obtained from single crystal data of their corresponding complexes (Supporting Information).[24,25] All computations were calculated by PC GAMESS.

Luminescence lifetimes were obtained with a 355 nm light generated from the third-harmonic generator pump, which used the pulsed Nd:yttrium aluminum garnet (YAG) laser as the excitation source. The Nd:YAG laser possesses a line width of 1.0 cm^{-1}, a pulse duration of 10 ns, and a repetition frequency of 10 Hz. A Rhodamine 6G dye pumped by the same Nd:YAG laser was used as the frequency-selective excitation source. All photoluminescence (PL) spectra were measured with a Hitachi F-4500 fluorescence spectrophotometer from 20 wt % Cu(I) complexes doped poly(methyl methacrylate) (PMMA) films. UV−visible absorption spectra were recorded using a Shimadzu UV-3101PC spectrophotometer. ^{1}H and ^{31}P NMR spectra were obtained with a Varian INOVA 300 spectrometer. Thermogravimetric analysis (TGA) was performed on a PerkinElmer thermal analyzer. Cyclic voltammetry measurements were conducted on a CHI660C electrochemical workstation, using a polished Pt plate as the working electrode, Pt mesh as the counter electrode, and a saturated calomel electrode (SCE) as the reference electrode, at a scan rate of 0.1 V/s. Voltammograms were recorded using freshly distilled CH_3CN solutions with $\sim 10^{-3}$ M samples and 0.1 M tetrabutylammonium hexafluorophosphate as the supporting electrolyte. Solutions were purged with N_2 for 10 min to remove dissolved O_2. Single crystal data were collected on a Siemens P4 single-crystal X-ray diffractometer with a Smart CCD-1000 detector and graphite-monochromated Mo Kα radiation, operating at 50 kV and 30 A at 298 K. All hydrogen atoms were calculated. All layers in OLEDs were deposited onto precleaned ITO substrates (resistivity <30 Ω, active area = 4 mm^2) by a resistive heating method under a chamber pressure of $\sim 3 \times 10^{-4}$ Pa. All measurements were carried out in air at room temperature without being specified.

Results and Discussion

Diimine Ligands. Our initial effort focuses on the selection of diimine ligands with high-π^*. In Sakaki's simplified model for the $[Cu(N-N)(P-P)]^+$ system, the excited electron is localized on the diimine ligand π^*_1 orbital, and electron configuration of the MLCT excited state can be represented as $(d_{xz})^1(\pi^*_1)^1$.[26] Considering that the π^*_1 orbital is antibonding between a C atom and coordination N atom (C=N bond), it is thus expected that the introduced electron donors taking the α and/or α' positions of C=N bond may improve π^*_1 more efficiently. Because a ligand steric effect leads to photophysical property variation of corresponding $[Cu(N-N)(P-P)]^+$ complexes, here, aiming at the confirmation of diimine ligand high-π^* effect on improving LUMO, electron-donors of N and/or S atoms are introduced into the α-position of a C=N bond as

TABLE 1: Photophysical Properties for Cu(I) Complexes

[Cu(N−N)(POP)]BF_4 N−N =	λ_{edg}[a] (nm)	λ_{em}[b] (nm)	τ[c] (μs)	Φ[d]
Bimda	363	470	2.1	0.08
Tbzimda	396	515	7.0	0.15
Et-Tbzimda	400	525	16.1	0.34
Pbzimda	503	560	2.6	0.09

[a] Values obtained in CH_2Cl_2 (1×10^{-5} mol/L), ± 1 nm. [b] Values obtained in PMMA films, ± 1 nm. [c] Values obtained in PMMA films, ± 5%. [d] Values obtained in PMMA films, ± 8%.

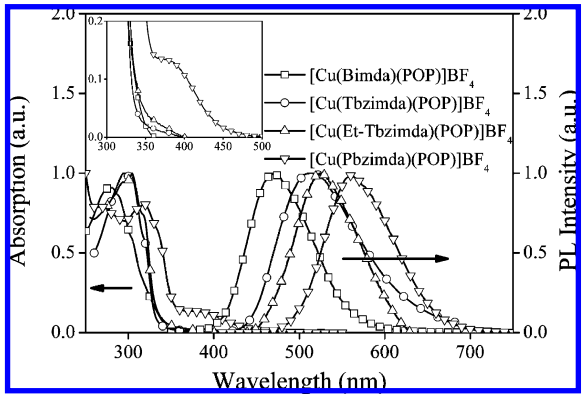

Figure 1. UV−vis absorption (in CH_2Cl_2 with a concentration of 1×10^{-5} mol/L) and PL spectra (in 20 wt % doped PMMA films) for Cu(I) complexes. Inset shows a magnified view of their absorption edges.

depicted in Scheme 1, where the introduced electron donors are far away from coordination N atoms so that the potential steric effect can be minimized. For comparison purposes, Pbzimda, having less electron donor N atoms in its molecule, is selected to be a reference ligand so that the diimine ligand high-π* effect on improving the LUMO of the corresponding [Cu(N−N)(P−P)]$^+$ complex can be further confirmed.

DFT calculation shows that ligand π values for Bimda, Tbzimda, Et-Tbzimda, and Pbzimda are −5.32, −5.59, −5.53, and −5.84 eV, respectively, while, π* values are −0.23, −1.21, −1.20, and −1.43 eV, respectively. It is observed that Bimda has the highest π* value, clearly due to the introduced electron donors and limited conjugation system. With the enlarged conjugation system caused by the coplanar phenyl ring, π* values of Tbzimda and Et-Tbzimda are largely lowered. As for Pbzimda, the π* value is further decreased because there is only one electron donor of a N atom within its molecule. As we mentioned, the [Cu(N−N)(P−P)]$^+$ complex HOMO is largely immune to the diimine ligand electronic effect because HOMO is dominated by contributions from the Cu(I) center and phosphorus ligand, while LUMO is controlled by the diimine ligand π*. It is thus expected that the [Cu(N−N)(POP)]BF_4 absorption edge, which corresponds to a HOMO→LUMO transition should follow the diimine ligands π* variation trend, where N-N = Bimda, Tbzimda, Et-Tbzimda, and Pbzimda.

Photophysical Properties of [Cu(N−N)(POP)]BF_4. Photophysical properties for [Cu(N−N)(POP)]BF_4, including absorption edges (λ_{edg}), emission peaks (λ_{em}), excited state lifetimes (τ), and PL quantum efficiencies (Φ), are measured and summarized in Table 1. UV−vis absorption and PL spectra for [Cu(N−N)(POP)]BF_4 shown in Figure 1 suggest that all [Cu(N−N)(POP)]BF_4 complexes demonstrate wide energy gaps (ΔE_g) between HOMO and LUMO, except for the reference ligand-based complex of [Cu(Pbzimda)(POP)]BF_4. It is notable that the absorption spectrum for [Cu(Bimda)(POP)]BF_4 ends at a remarkably short wavelength of 363 nm, with a high-energy emission peaking at 470 nm, which is by now shorter than those of any other reported [Cu(diimine ligand)(POP)]$^+$ complexes. In Wang's constructive study on highly efficient [Cu(diimine ligand)(POP)]BF_4 emitters, two bulky alkyl moieties were introduced into the 2- and 9-positions of the 1,10-phenanthroline ligand so that the MLCT excited state geometry distortion can be suppressed, resulting in efficient green emitters peaking at ∼520 nm.[27] However, unlike emitters reported by Wang, no additional sterically blocking moiety is introduced into [Cu(Bimda)(POP)]BF_4. Thus, the high-energy emission of [Cu(Bimda)(POP)]BF_4 is completely attributed to its wide energy gap between HOMO and LUMO. All [Cu(N−N)(POP)]BF_4 complexes exhibit broad emissions, without giving any vibronic progressions, suggesting that the emissive excited states have a CT character.[28] Combined with their long excited-state lifetimes, the emissions are thus attributed to emissive excited states of ^{3}MLCT. Here, high-energy emission from the [Cu(N−N)(POP)]BF_4 ^{3}MLCT excited state is realized by the utilization of the diimine ligand with high-π*.

On the other hand, as for [Cu(Pbzimda)(POP)]BF_4 which owns the lowest diimine ligand π*, the low-energy absorption band extends to visible region (∼500 nm), with a yellow-region emission peaking at 560 nm. Diimine ligand high-π* effect on improving LUMO is thus the first step confirmed by the large $\lambda_{edg}/\lambda_{em}$ difference between [Cu(Pbzimda)(POP)]BF_4 and [Cu(Bimda/ Tbzimda/ Et-Tbzimda)(POP)]BF_4. It is observed that [Cu(N−N)(POP)]BF_4 $\lambda_{edg}/\lambda_{em}$ variation trends ([Cu(Bimda)(POP)]BF_4 < [Cu(Tbzimda)(POP)]BF_4 < [Cu(Pbzimda)(POP)]BF_4) correlate well with π* value variation trends of corresponding diimine ligands (Bimda > Tbzimda > Pbzimda) as we supposed, indicating that [Cu(N−N)(POP)]BF_4 ΔE_g is apparently dominated by diimine ligand π*.

Confirmation of the Diimine Ligand High-π* Effect on Improving LUMO. ***Comparison between [Cu(Et-Tbzimda)(POP)]BF_4 and [Cu(Pbzimda)(POP)]BF_4.*** The favorable role played by the diimine ligand with high-π* is clearly established when we compare [Cu(Et-Tbzimda)(POP)]BF_4 and [Cu(Pbzimda)(POP)]BF_4. The reference ligand, Pbzimda, has a similar molecular structure to that of Et-Tbzimda, resulting in similar static congestions in their corresponding [Cu(N−N)(POP)]BF_4 complexes, but the diimine ligands π* values are different, which provides a possibility to further confirm the diimine ligand high-π* effect on improving the LUMO of the corresponding [Cu(N−N)(POP)]BF_4 complex.

It is no surprise that the crystal structures of [Cu(Et-Tbzimda)(POP)]BF_4 and [Cu(Pbzimda)(POP)]BF_4 shown in Figure 2 confirm that the Cu(I) center in both complexes has a widely reported distorted tetrahedral geometry (see Supporting Information for detailed crystallographic data). Their geometric parameters are summarized in Table 2. The dihedral angles between N1−Cu−N2 and P1−Cu−P2 planes are measured to be 89.11° for [Cu(Et-Tbzimda)(POP)]BF_4 and 89.68° for [Cu(Pbzimda)(POP)]BF_4. Cu−N bond lengths localize in a region of 2.04−2.16 Å, which are comparable with the literature values.[19−22] Cu−P bond lengths are similar to each other. As for the bond angles of N1−Cu−N2 and P1−Cu−P2, which may influence the MLCT excitation energy of the corresponding [Cu(N−N)(POP)]$^+$ complex, no obvious difference between [Cu(Et-Tbzimda)(POP)]BF_4 and [Cu(Pbzimda)(POP)]BF_4 is observed.[28] Thus, we come to the conclusion that the large λ_{edg} difference between [Cu(Et-Tbzimda)(POP)]BF_4 and [Cu(Pbzimda)(POP)]BF_4 is not caused by their structural distinctness but by their electronic distinctness originating from the diimine ligands.

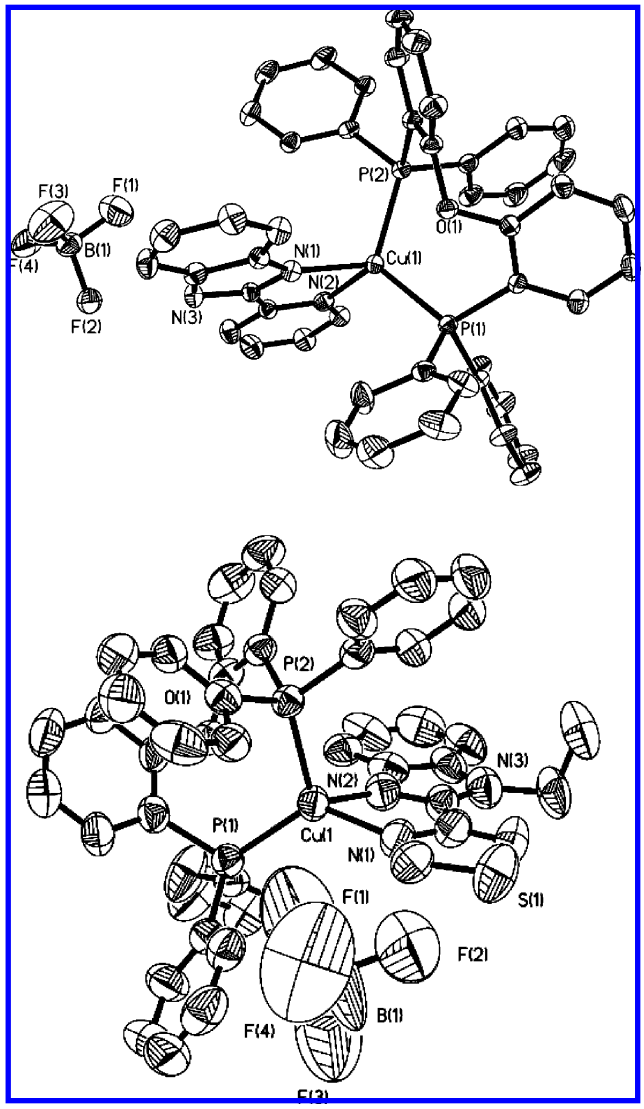

Figure 2. Crystal structures of $[Cu(Et\text{-}Tbzimda)(POP)]BF_4$ (top) and $[Cu(Pbzimda)(POP)]BF_4$ (bottom).

TABLE 2: Selected Geometric Parameters of $[Cu(Et\text{-}Tbzimda)(POP)]BF_4$ and $[Cu(Pbzimda)(POP)]BF_4$

	$[Cu(Et\text{-}Tbzimda)(POP)]BF_4$	$[Cu(Pbzimda)(POP)]BF_4$
Cu(1)−N(1)	2.157(6)	2.078(4)
Cu(1)−N(2)	2.042(6)	2.122(4)
Cu(1)−P(1)	2.229(2)	2.2482(13)
Cu(1)−P(2)	2.2812(19)	2.2554(13)
Cu···O	3.115	3.031
N(1)−Cu−N(2)	79.1(3)	79.87(15)
N(1)−Cu−P(1)	125.69(18)	113.28(11)
N(2)−Cu−P(1)	119.18(18)	115.68(11)
N(1)−Cu−P(2)	107.98(17)	112.21(11)
N(2)−Cu−P(2)	106.36(19)	115.26(11)
P(1)−Cu−P(2)	113.19(7)	115.50(5)

In order to gain a further understanding of their electronic nature, TD-DFT, which has proven to be a powerful tool when exploring molecular excited state properties, is performed on $[Cu(Et\text{-}Tbzimda)(POP)]BF_4$ and $[Cu(Pbzimda)(POP)]BF_4$.[22] Table 3 presents the percentage composition of their frontier molecular orbitals as well as their singlet excitations ($S_0 \rightarrow S_1$). Similarly, as depicted by Figure 3, both HOMOs are dominated by contributions from the Cu(I) center and POP ligand, while both LUMOs are essentially π^* of their corresponding diimine ligands. At the same time, the HOMO value demonstrates a small variation with different diimine ligands. However, the LUMO value is more sensitive to diimine ligand variation as shown in Table 3. Because the Et-Tbzimda π^* value is higher than that of Pbzimda, it is reasonable to observe that the $S_0 \rightarrow S_1$ excitation energy of $[Cu(Et\text{-}Tbzimda)(POP)]BF_4$ is higher than that of $[Cu(Pbzimda)(POP)]BF_4$, which is consistent with the shorter λ_{edg} for $[Cu(Et\text{-}Tbzimda)(POP)]BF_4$ compared with that of $[Cu(Pbzimda)(POP)]BF_4$.

TABLE 3: Calculated Percentage Composition of Cu(I) Complexes Frontier Molecular Orbitals and Their Singlet Excitations at RB3PW91/SBKJC Level

	$[Cu(Et\text{-}Tbzimda)(POP)]BF_4$	$[Cu(Pbzimda)(POP)]BF_4$
HOMO	Cu (20.6%) POP (63.4%) −7.60 eV	Cu (22.6%) POP (60.6%) −7.77 eV
LUMO	Et-Tbzimda (88.8%) −4.65 eV	Pbzimda (92.0%) −5.11 eV
$S_0 \rightarrow S_1$	HOMO→LUMO (99.1%) 2.33 eV	HOMO→LUMO (92.3%) 1.74 eV

Electrochemistry Study on $[Cu(N-N)(POP)]BF_4$. Electrochemical data should provide direct evidence for HOMO and LUMO variation of the four $[Cu(N-N)(POP)]BF_4$ complexes. As shown in Table 4, the LUMO value varies dramatically from −3.22 eV for $[Cu(Pbzimda)(POP)]BF_4$ to −2.34 eV for $[Cu(Bimda)(POP)]BF_4$, while HOMO values localize in a narrow region of −5.51 to −5.31 eV (see Supporting Information for a detailed presentation). The electrochemistry measured HOMO and LUMO variation trends are consistent with the above theoretical analysis on HOMO and LUMO values. Furthermore, it is observed that LUMO value variation trends observed from electrochemical data {$[Cu(Bimda)(POP)]BF_4$ > $[Cu(Tbzimda)(POP)]BF_4$ > $[Cu(Pbzimda)(POP)]BF_4$} also correlate with π^* value variation trends of their corresponding diimine ligand (Bimda > Tbzimda > Pbzimda), which can be explained as follows. Both our theoretical calculation and literature results suggest that the $[Cu(N-N)(P-P)]^+$ complex HOMO is dominated by contributions from the Cu(I) center and phosphorus ligand, while LUMO is essentially dominated by the diimine ligand π^*.[22,26] With diimine ligand variation, HOMO is nearly unaffected as well as its value. However, LUMO varies dramatically with different diimine ligands, and its value is also controlled by the diimine ligand π^*, resulting in the highly restricted HOMO values and largely variable LUMO values. Thus, the diimine ligand high-π^* effect on improving LUMO is fully confirmed here by theoretical and experimental results.

Electroluminescence Performances. TGA results shown in Table 4 confirm that all four $[Cu(N-N)(POP)]BF_4$ complexes have high decomposition temperatures (T_{dec}, see Supporting Information for a detailed presentation) around 300 °C, suggesting that they are all thermally stable enough for OLED device fabrication through the resistive heating method under vacuum.[11] Considering their promising PL quantum efficiencies and short excited-state lifetimes, blue-emitting $[Cu(Bimda)(POP)]BF_4$ and green-emitting $[Cu(Et\text{-}Tbzimda)(POP)]BF_4$ are selected for OLED fabrication. The OLEDs utilizing $[Cu(Bimda)(POP)]BF_4$ and $[Cu(Et\text{-}Tbzimda)(POP)]BF_4$ as dopants in a CBP emissive layer were fabricated with a general structure of ITO/*m*-MTDATA (30 nm)/NPB (20 nm)/CBP:Cu(I) complex (wt %, 30 nm)/Bphen (20 nm)/AlQ (20 nm)/LiF/Al, where *m*-MTDATA is used as the hole injection layer and NPB is the hole-transporting layer. Meanwhile, Bphen and AlQ are employed as the exciton-blocking layer and the electron-transporting layer, respectively. The optimal dopant concentrations were found to be 23% for $[Cu(Bimda)(POP)]BF_4$ and 18% for $[Cu(Et\text{-}Tbzimda)(POP)]BF_4$.

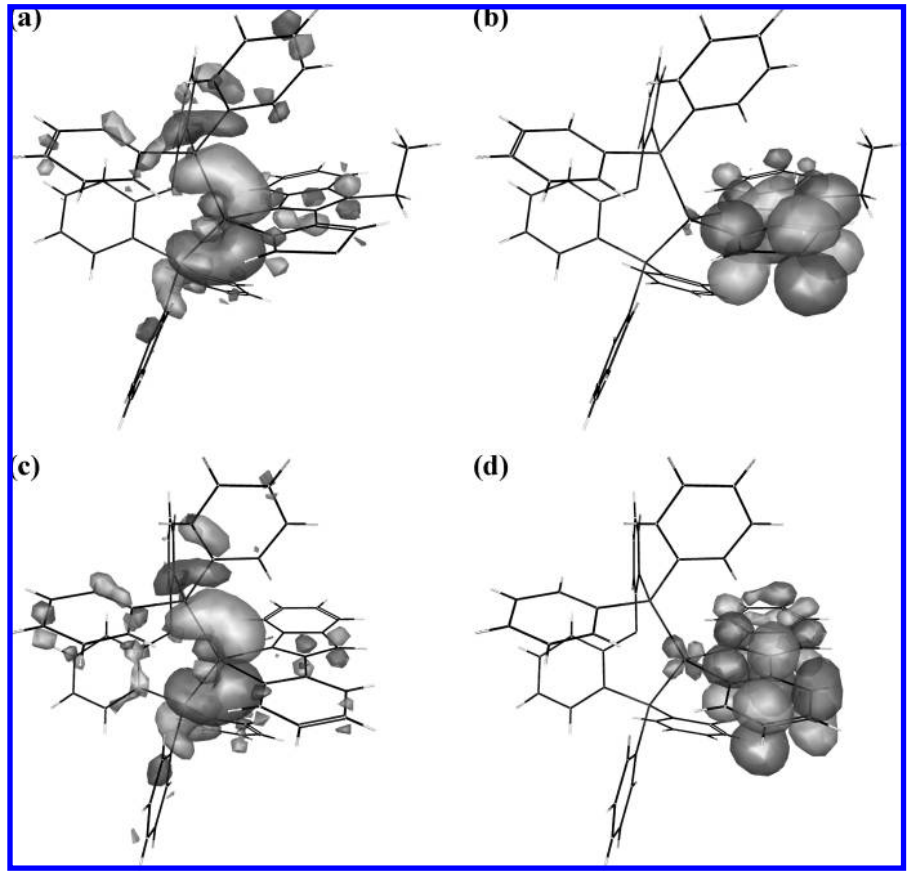

Figure 3. (a) Graphic presentation of [Cu(Et-Tbzimda)(POP)]BF_4 HOMO. (b) Graphic presentation of [Cu(Et-Tbzimda)(POP)]BF_4 LUMO. (c) Graphic presentation for [Cu(Pbzimda)(POP)]BF_4 HOMO. (d) Graphic presentation for [Cu(Pbzimda)(POP)]BF_4 LUMO. All graphics are calculated at B3PW91/SBKJC level. BF_4^- is not given in any graphic to provide a clear view.

TABLE 4: Electrochemistry Measured HOMO and LUMO Values and Decomposition Temperatures of Cu(I) Complexes

[Cu(N−N)(POP)]BF_4 N−N =	HOMO[a] (eV)	LUMO[a] (eV)	T_{dec}[b] (°C)
Bimda	−5.31	−2.34	289
Tbzimda	−5.46	−2.56	306
Et-Tbzimda	−5.45	−2.58	335
Pbzimda	−5.51	−3.22	356

[a] Values ± 8%. [b] Defined as the temperature of 10% weight loss.

Figure 4 shows the emission spectra of EL devices at applied voltages of 15 V for a [Cu(Bimda)(POP)]BF_4-based device and 12 V for a [Cu(Et-Tbzimda)(POP)]BF_4-based device. The EL emissions peaking at 480 and 532 nm originating from Cu(I)-dopants demonstrate a slight red shift compared with their corresponding PL spectra, which is caused by the intermolecular interaction between dopant and host.[9] The maximum brightness achieved from a [Cu(Bimda)(POP)]BF_4-based device is as high as 2850 cd/m^2 at 15 V. Meanwhile, a [Cu(Et-Tbzimda)(POP)]-BF_4-based device reaches a maximum EL brightness of 2320 cd/m^2 at 12 V.

Characteristics of EL efficiency versus current density are presented in Figure 5. The peak EL efficiency for a [Cu(Bimda)-(POP)]BF_4-based device (1.47 cd/A) is found to be lower than that for a [Cu(Et-Tbzimda)(POP)]BF_4-based device (2.35 cd/A), clearly due to the largely smaller quantum efficiency of [Cu(Bimda)(POP)]BF_4 than that of [Cu(Et-Tbzimda)(POP)]BF_4. However, a [Cu(Bimda)(POP)]BF_4-based device EL efficiency remains 90% of its maximum at a high current density of 100 mA/cm^2, demonstrating no obvious triplet−triplet (T-T)

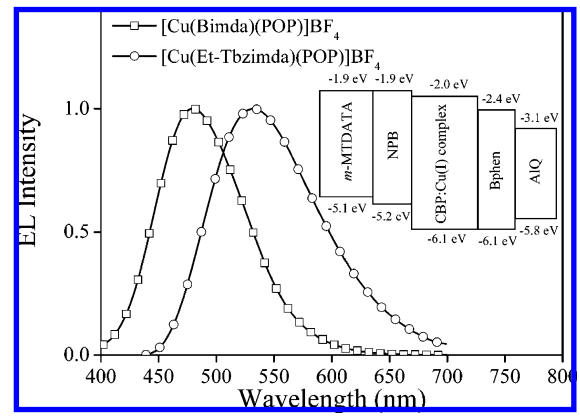

Figure 4. EL spectra at applied voltages of 15 V for a [Cu(Bimda)-(POP)]BF_4-based device and 12 V for a [Cu(Et-Tbzimda)(POP)]BF_4-based device. Inset shows a general device structure.

annihilation effect.[29] However, it appears that a [Cu(Et-Tbzimda)-(POP)]BF_4-based device suffers badly from T-T annihilation due to the long excited-state lifetime of the emitter. EL efficiency decreases dramatically as current density increases, and only 38% of its maximum EL efficiency remains at the current density of 100 mA/cm^2. EL efficiencies and brightness of blue-emitting and green-emitting devices are among the highest reported for the Cu(I) emitter-based EL devices, making [Cu(Bimda)(POP)]BF_4 and [Cu(Et-Tbzimda)(POP)]BF_4 promising candidates for OLED applications.

Conclusion

In this paper, we propose a potential method leading to high-energy emitting Cu(I) complexes. Diimine ligands with high-

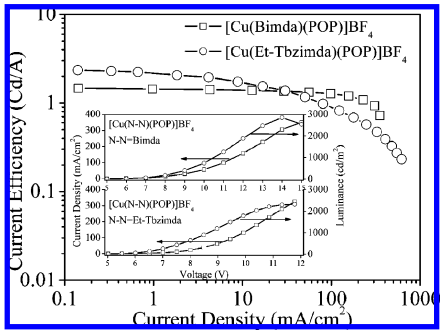

Figure 5. Device characteristics of EL efficiency versus current density. Inset shows luminance and current density characteristics with various voltages.

π^* and their corresponding $[Cu(N-N)(POP)]BF_4$ complexes are synthesized. Systematic research proves that the utilization of diimine ligands with high-π^* is an effective method leading to high-energy emission from $[Cu(N-N)(POP)]BF_4$ complexes. Efficient blue- and green-emitters are realized, and their electroluminescence performances are also investigated. A maximum brightness of 2850 cd/m^2 is achieved for the blue-emitting EL device, with an emission peaking at 480 nm. Meanwhile, the green-emitting EL device reaches a maximum brightness of 2320 cd/m^2, with an emission peaking at 532 nm.

Acknowledgment. The authors are gratefully for the financial support of the One Hundred Talents Project from the Chinese Academy of Sciences and the National Natural Science Foundations of China (Grant 50872130).

Supporting Information Available: Detailed crystallographic data of $[Cu(Et\text{-}Tbzimda)(POP)]BF_4$ and $[Cu(Pbzimda)(POP)]BF_4$, a detailed presentation of cyclic voltammograms and TGA of $[Cu(N-N)(POP)]\ BF_4$ (in PDF format), where N−N = Bimda, Tbzimda, Et-Tbzimda, and Pbzimda, and crystallographic files of $[Cu(Et\text{-}Tbzimda)(POP)]BF_4$ and $[Cu(Pbzimda)(POP)]BF_4$ (in CIF format). This information is available free of charge via the Internet at http://pubs.acs.org.

References and Notes

(1) Armaroli, N.; Accorsi, G.; Cardinali, F.; Listorti, A. *Top. Curr. Chem.* **2007**, *280*, 69.

(2) Lavie-Cambot, A.; Cantuel, M.; Leydet, Y.; Jonusauskas, G.; Bassani, D. M.; McClenaghan, N. D. *Coordin. Chem. Rev.* **2008**, *252*, 2572.

(3) Tsuboyama, A.; Kuge, K.; Furugori, M.; Okada, S.; Hoshino, M.; Ueno, K. *Inorg. Chem.* **2007**, *46*, 1992.

(4) Aslanidis, P.; Cox, P. J.; Davanidis, S.; Tsipis, A. C. *Inorg. Chem.* **2002**, *41*, 6875.

(5) Fournier, E.; Lebrun, F.; Drouin, M.; Decken, A.; Harvey, P. D. *Inorg. Chem.* **2004**, *43*, 3127.

(6) Harvey, P. D.; Drouin, M.; Zhang, T. *Inorg. Chem.* **1997**, *36*, 4998.

(7) Kirchhoff, J. R.; McMillin, D. R.; Robinson, W. R.; Powell, D. R.; Mckenzie, A. T.; Chen, S. *Inorg. Chem.* **1985**, *24*, 3928.

(8) Palmer, C. E. A.; McMillin, D. R. *Inorg. Chem.* **1987**, *26*, 3837.

(9) Che, G.; Su, Z.; Li, W.; Chu, B.; Li, M.; Hu, Z.; Zhang, Z. *Appl. Phys. Lett.* **2006**, *89*, 103511.

(10) Xia, H.; He, L.; Zhang, M.; Zeng, M.; Wang, X. M.; Lu, D.; Ma, Y. G. *Opt. Mater.* **2007**, *29*, 667.

(11) Zhang, Q. S.; Ding, J. Q.; Cheng, Y. X.; Wang, L. X.; Xie, Z. Y.; Jing, X. B.; Wang, F. S. *Adv. Funct. Mater.* **2007**, *17*, 2983.

(12) Feng, Q.; Li, D.; Yin, Y. G.; Feng, X. L.; Cai, J. W. *Acta Chim. Sinica* **2002**, *60*, 2167.

(13) McMillin, D. R.; McNett, K. M. *Chem. Rev.* **1998**, *98*, 1201.

(14) Armaroli, N. *Chem. Soc. Rev.* **2001**, *30*, 113.

(15) Scaltrito, D. V.; Thompson, D. W.; O'Callaghan, J. A.; Meyer, G. J. *Coord. Chem. Rev.* **2000**, *208*, 243.

(16) Eggleston, M. K.; McMillin, D. R.; Koenig, K. S.; Pallenberg, A. J. *Inorg. Chem.* **1997**, *36*, 172.

(17) Cunningham, C. T.; Cunningham, K. L. H.; Michalec, J. F.; McMillin, D. R. *Inorg. Chem.* **1999**, *38*, 4388.

(18) Rader, R. A.; McMillin, D.; Buckner, M. T.; Matthews, T. G.; Casadonte, D. J.; Lengel, R. K.; Whittaker, S. B.; Darmon, L. M.; Lytle, F. E. *J. Am. Chem. Soc.* **1981**, *103*, 5906.

(19) M^{c}Cormick, T.; Jia, W. L.; Wang, S. *Inorg. Chem.* **2006**, *45*, 147.

(20) Cuttell, D. G.; Kuang, S. M.; Fanwick, P. E.; McMillin, D. R.; Walton, R. A. *J. Am. Chem. Soc.* **2002**, *124*, 6.

(21) Kuang, S. M.; Cuttel, D. G.; McMillin, D. R.; Fanwick, P. E.; Walton, R. A. *Inorg. Chem.* **2002**, *41*, 3313.

(22) Yang, L.; Feng, J. K.; Ren, A. M.; Zhang, M.; Ma, Y. G.; Liu, X. D. *Eur. J. Inorg. Chem.* **2005**, *10*, 1867.

(23) Thummel, R. P.; Goulle, V.; Chen, B. *J. Org. Chem.* **1989**, *54*, 3057.

(24) Haj, M. A.; Quiros, M.; Salas, J. M. *J. Chem. Cryst.* **2004**, *34*, 549.

(25) Ma, R.; Muir, M. M.; Cadiz, M. E.; Muir, J. A. *Acta Crystallogr., Sect. C* **1991**, *47*, 1539.

(26) Sakaki, S.; Mizutani, H.; Kase, Y. I. *Inorg. Chem.* **1992**, *31*, 4575.

(27) Zhang, Q. S.; Zhou, Q. G.; Cheng, Y. X.; Wang, L. X.; Ma, D. G.; Jing, X. B. *Adv. Mater.* **2004**, *16*, 432.

(28) McCormick, T.; Jia, W. L.; Wang, S. *Inorg. Chem.* **2006**, *45*, 147.

(29) Baldo, M. A.; Adachi, C.; Forrest, S. R. *Phys. Rev. B* **2000**, *62*, 10967.

JP903774G